Acta Geotechnica (2021) 16:3813–3830
https://doi.org/10.1007/s11440-021-01376-6

RESEARCH PAPER

An effective stress-based DSC model for predicting the coefficient of lateral soil pressure in unsaturated soils

Amir Akbari Garakani[1] · Ali Pirjalili[2] · Chandrakant S. Desai[3]

Received: 11 March 2021 / Accepted: 30 September 2021 / Published online: 15 October 2021

Abstract

In this study, an analytical model is developed to establish a framework for predicting the coefficient of lateral soil pressure in unsaturated soils. To this end, the disturbed state concept (DSC) is implemented along with the concept of effective stress for unsaturated soils. Accordingly, upper and lower limits are considered for the structural disturbance of the soil during hydromechanical loading, and a suction-dependent analytical framework is proposed for calculating continuous variations of the coefficient of lateral soil pressure, from the at-rest to active state of the soil, against the effective vertical stress parameter. The functionality of the proposed model is verified against experimental results obtained from a series of laboratory unsaturated drained tests conducted on two different soil materials (a Sand–Kaolin mixture and Firouzkouh Clay) with two initial void ratios. Quantitative comparisons show excellent conformance between the predicted and experimental data. A practical example of calculating lateral soil pressure on a gravity retaining wall is also presented, in which the results obtained from the model presented in this study and the conventional classic approach of calculating the lateral soil pressure on retaining walls are compared. It is hoped that the results of this study can help researchers and designers to obtain improved values of lateral soil pressure in unsaturated soil.

Keywords Analytical model · Disturbed state concept · Effective stress · Experimental verification · Lateral soil pressure · Unsaturated soils

List of symbols

a, z, D_u	DSC-model parameters
a_o, C_a	Fitting parameters for predicting a
C_{Du}	Fitting parameter for predicting D_u
D	Disturbance parameter
e	Void ratio of the soil
e_o	Initial void ratio of the soil
F_h	Overall lateral force
GWL	Ground water level
h_{unsat}	Wall height or height of the unsaturated backfill soil
h_w	Elevation above GWL
i	Numeral
k	Coefficient of the lateral soil pressure
k_{a}	Coefficient of the lateral soil pressure in the active condition
$k_{\mathrm{experimental}}$	Experimental value of k
k_{FA}	k Value corresponding to zero matric suction
$k_{\mathrm{predicted}}$	Model-predicted value of k
k_o	Coefficient of the lateral soil pressure in the at-rest condition
k_{ou}	Unsaturated at-rest coefficient of the lateral soil pressure
k_{RI}	k Value corresponding to the maximum applied matric suctions
k_ψ	Coefficient of the lateral soil pressure at a given matric suction

✉ Amir Akbari Garakani
aakbari@nri.ac.ir

Ali Pirjalili
a.pirjalili@modares.ac.ir

Chandrakant S. Desai
csdesai@email.arizona.edu

[1] Power Industry Structures Research Department, Niroo Research Institute, Room 403, 4th Floor, At the end of Dadman Blvd., Shahrak Gharb, Postal Box: 14665517, Postal Code:1468617151 Tehran, Iran

[2] The Faculty of Civil and Environmental Engineering, Tarbiat Modares University, Tehran, Iran

[3] Regents Professor (Emeritus), Department of Civil and Arch. Eng. and Mechanics, Univ. of Arizona, Arizona, USA

Max ($k_{experimental}$)	Maximum of the experimental k values
Min ($k_{experimental}$)	Minimum of the experimental k values
N	Number of data in each data set
NRMSE	Normalized root mean square error
P_{FA}	The soil mechanical response at the FA state
P_{Int}	Soil mechanical response at the intermediate phase of disturbance
P_{RI}	Soil mechanical response at the RI state
RMSE	Root mean square error
S_r	Degree of saturation of the soil
S_{ro}	Degree of saturation of the soil at zero matric suction
$S_{r(RI)}$	Degree of saturation of the soil at RI condition
$S_{r(\psi)}$	Degree of saturation of the soil at a given matric suction
u_a	Pore air pressure
u_w	Pore water pressure
x	An independent typical variable
z_o, C_z	Fitting parameters for predicting z
Δe	Changes in void ratio
α, m, n	Fitting parameters of the van Genuchten's suggested model for SWRC
χ	Effective stress parameter in unsaturated soils
$d\varepsilon_v$	Increment of plastic volumetric strain
ε_e	Elastic volume strain
ε_r	Radial (lateral) strain
ε_v	Total volumetric strain
γ	Soil density
γ_w	Water density
σ	Total stress
σ'	Effective stress
σ_h	Net horizontal stress
σ'_h	Effective horizontal stress
σ_v	Net vertical stress
σ'_v	Effective vertical stress
σ_{net}	Net stress
σ_s	Suction-stress
σ_v	Net vertical stress
ψ	Matric suction
ζ_v	Accumulative plastic volumetric strain

1 Introduction and background

The coefficient of lateral soil pressure, k, is a key factor in the analysis of many geotechnical problems, *e.g.,* underground structures, slope stability, retaining walls, etc. Due to the dependence of this parameter on several state variables or material parameters, its precise and accurate determination is very challenging, especially in unsaturated soils.

Many studies have been conducted to examine k for saturated soils [3, 5, 22, 23, 34, 35, 37, 40, 46]. For example, Mayne and Kulhawy [34] performed a comprehensive study on the dependency of the at-rest soil pressure on the over consolidation ratio and reviewed plenty of experimental data reported by different researchers. However, there are very few investigations on the coefficient of lateral soil pressure and its relevant state variables (or parameters) for *unsaturated* soils, either experimentally [1, 27, 36, 39, 41, 45, 49, 51], analytically [29, 30, 44, 47, 50] or numerically [13, 26, 28]. As previous studies have shown, the lateral soil pressure in unsaturated soils is remarkably affected by the soil type [28, 41], the initial soil saturation, S_r, or the matric suction, ψ, [1, 13, 27, 30, 36, 39, 41, 45, 49, 51], the stress state within the soil [1, 13, 30, 41, 51], the climate parameters (*e.g.,* infiltration or evaporation) [44, 45, 47] and the geometrical aspects of the retaining structure that supports the soil against lateral deformations [28, 29]. In general, it has been indicated that the at-rest and the active soil pressure coefficients (k_{ou} and k_{au}, respectively) increase by increasing the degree of saturation of the soil and the principal stress level within the soil body, or by decreasing the matric suction of the soil. In addition, it was found that the higher the soil density, the less the lateral soil pressure in unsaturated soil deposits.

Among the limited studies on assessing lateral soil pressure in unsaturated soils, only the at-rest or the active coefficients of lateral soil pressure were studied, and the *continuous* variation of the unsaturated lateral soil pressure from the *at-rest* to the *active* state of the examined soils has not been investigated.

In this research, a suction-dependent effective stress-based analytical framework is developed on the basis of the disturbed state concept (DSC) to predict the continuous variation of unsaturated lateral soil pressure coefficient from the at-rest to the active state of the soil. DSC, well-known as a comprehensive method for predicting the mechanical behavior of geomaterials, was first proposed by Desai [6–9] and developed afterward by many researchers [10–12, 15, 17, 20]. According to the DSC, the mechanical response of soil due to changing state variables can be defined by considering the soil response in two extreme

soil structural reference conditions, namely *the relative intact soil structure* (RI) and *the fully adjusted soil structure* (FA).

To assess the functionality of the proposed analytical model, the analytical results from this research are compared quantitatively with data obtained from the experimental study by Pirjalili et al. [41]. In that study, a series of twenty suction-controlled drained tests were conducted on two different unsaturated soils using a suction-controlled ring device under five different matric suctions. This device is capable of continuously measuring the unsaturated lateral soil pressure and corresponding lateral (radial) strain, ε_r, as well as controlling the matric suction and measuring the water content of the soil specimens during the tests. In addition to the data reported by Pirjalili et al. [41], a complementary series of experimental tests were performed to measure the lateral soil pressure changes in fully saturated (*i.e.,* 0-kPa matric suction) soil conditions.

2 Development of the analytical solution

In this research, an analytical solution has been developed to predict the variation of the coefficient of lateral soil pressure in unsaturated soils in terms of the state variables and soil parameters that influence the behavior. Also, the disturbed state concept (DSC) and the effective stress approach for unsaturated soils are considered simultaneously.

2.1 Lateral soil pressure in unsaturated soils in terms of effective stress

Generally, the coefficient of lateral soil pressure, k, should be calculated from the effective vertical stress and the effective horizontal stress, as shown by Eq. (1):

$$k = \frac{\sigma'_{\mathrm{h}}}{\sigma'_{\mathrm{v}}} \tag{1}$$

where σ'_{h} and σ'_{v} are the effective horizontal and the effective vertical stresses, respectively. The single-phase effective stress relationship in unsaturated soils was first formulated by Bishop [2], as:

$$\sigma' = (\sigma - u_a) + \chi \times (u_a - u_w) = \sigma_{\mathrm{net}} + \chi \times \psi = \sigma_{\mathrm{net}} + \sigma_s \tag{2}$$

where σ', σ, σ_{net}, ψ, u_a, u_w, χ and σ_s are effective stress, total stress, net stress, matric suction, pore air pressure, pore water pressure, effective stress parameter and suction-stress, respectively. There has been a long-running debate on the nature and determination of χ· χ is a function of soil saturation and reflects the contribution of matric suction to effective stress; it is an average weighing factor reflecting the inter-particle capillary as well as physico-chemical forces [33]. In an unsaturated state of the soil, χ typically varies between zero (in fully dry conditions) to unity (in fully saturated conditions). Many relationships have been reported by researchers to show the dependency of χ on soil saturation [14, 16, 19, 21, 24, 25, 31, 38, 48]. For instance, it is suggested that χ can be simply taken as the degree of saturation, S_r, [4, 24, 43] or as the effective saturation, S_e, [14, 16, 19, 21].

In accordance with Eq. (2), effective horizontal and vertical stresses can be attained by Eqs. (3a) and (3b), respectively:

$$\sigma'_h = \sigma_h + \chi \times (u_a - u_w) = \sigma_h + \sigma_s \tag{3a}$$

$$\sigma'_v = \sigma_v + \chi \times (u_a - u_w) = \sigma_v + \sigma_s \tag{3b}$$

where σ_{h} and σ_{v} are the net horizontal and net vertical stresses, respectively, that are conventionally controlled or measured during unsaturated tests. Therefore, by knowing the soil–water retention behavior (*i.e.,* Soil–Water Characteristic Curve, SWRC) and considering a suitable relationship for changing the effective stress parameter, χ, against the matric suction, ψ, it is possible to calculate the coefficient of lateral soil pressure, k, for unsaturated soils by implementing Eqs. (1) and (3).

2.2 Implementing the disturbed state concept (DSC) for calculating k

The DSC was first introduced by Desai [6–8] and extended by Geiser et al. [17] for constitutive modeling of unsaturated soils. Details of the DSC are presented by Desai [9]. As a constitutive framework, DSC defines the overall behavior of a deforming material in terms of the behavior of component materials with regards to continuum and disturbed states. The former is often denoted as *Relative Intact* (RI) and the latter as *Fully Adjusted* (FA).

Accordingly, the mechanical response of the soil in an *intermediate state*, P_{Int}, can be determined by knowing the two corresponding values in RI and FA states, namely P_{RI} and P_{FA}. Hence, in accordance with DSC, the expression for calculating P_{Int} is:

$$P_{\mathrm{Int}} = P_{\mathrm{RI}} - (P_{\mathrm{RI}} - P_{\mathrm{FA}}) \times D \tag{4}$$

Equation (4) provides a continuous expression to define P_{Int} in terms of P_{RI} and P_{FA}, in which, P_{RI} and P_{FA} are soil responses at RI and FA states, respectively, and D is a disturbance parameter. The disturbance parameter, D, defines the progression of degradation (softening) or healing and coupling between the RI and FA responses and varies between zero and unity during the RI toward the ultimate FA state. D is typically defined in the form of an

exponential function in terms of accumulative plastic volumetric strain, ζ_v, as shown by Eq. (5):

$$D = D_u\left(1 - e^{\left(-a\zeta_v^z\right)}\right) \tag{5}$$

In Eq. (5), D_u, a and z are model parameters that depend on the type of material and the loading conditions. In Fig. 1, variations of P_{Int}, P_{RI} and P_{FA} versus typical independent variable, x (*e.g.,* a stress state parameter), are shown schematically.

According to the basic concepts of DSC, the soil experiences the most structural disturbance in the *FA* state, in which the soil has the least stiffness. On the other hand, in the *RI* state, the soil experiences a gradual structural disturbance.

Unsaturated soils can be considered to be in the *FA* condition when the matric suction of the soil is zero and the soil is fully saturated. Moreover, since the soil stiffness is *relatively* the highest (compared to other cases) under maximum applied matric suction, unsaturated soils can be considered to be in the *RI* condition when maximum matric suction is applied to the soil.

In this research, the conceptual framework of DSC has been implemented to demonstrate the variations of the unsaturated coefficient of lateral soil pressure, k, in terms of the effective vertical stress, σ'_v. Accordingly, by considering the coefficient of the lateral soil pressure at a given matric suction, k_ψ, as P_{int} and considering k values corresponding to the 0-kPa and the maximum applied matric suctions as k_{FA} and k_{RI} in Eq. (4), respectively, a general formulation for calculating k at a given matric suction, ψ, is obtained, as shown by Eq. (6).

$$k_\psi = k_{\mathrm{RI}} - (k_{\mathrm{RI}} - k_{\mathrm{FA}}) \times D \tag{6}$$

In Eq. (6), k_{FA} and k_{RI} are two input parameters, whose variations against the effective vertical stress, σ'_v, must be known. Also, the disturbance parameter, D, is a function of three material parameters (namely, D_u, a and z), as previously denoted in Eq. (5). In this study, D_u, a and z are defined in terms of the applied matric suction to the soil, by considering the experimental unsaturated test results. Details are discussed in the following sections.

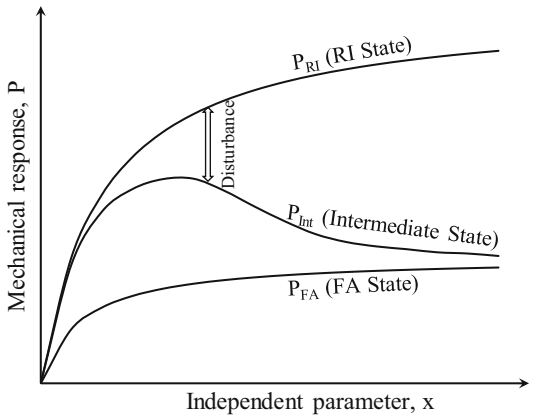

Fig. 1 Schematic of P_{Int}, P_{RI} and P_{FA}

3 Experimental data

In this research, the constitutive parameters of the proposed DSC model are calculated in accordance with the experimental data from Pirjalili et al. [41], who performed laboratory tests on two different unsaturated soils (namely, Firouzkouh Clay [CL] and Sand–Kaolin mixture [SC]), using a developed unsaturated suction-controlled ring device. Accordingly, reconstituted specimens of a Sand–Kaolin mixture (with two different initial void ratios, e_o, of 0.52 and 0.72) and a Firouzkouh Clay (with two different initial void ratios of 0.71 and 0.92) were tested under five different matric suctions (ψ = 10, 30, 50, 70 and 90 kPa) to examine the dependency of the unsaturated coefficient of lateral soil pressure on the void ratio and matric suction. Further details about the experimental work are available in [41, 42].

The soil water retention curves (SWRC) of the examined soil materials under wetting paths are shown in Fig. 2 along with the fitted curves and corresponding parameters obtained from van Genuchten's suggested model [18], as presented by Eq. (7):

$$\psi = \frac{S_{\mathrm{ro}}}{(1 + (\alpha\psi)^n)^m} \tag{7}$$

In Eq. (7), S_{ro} is the degree of saturation of the soil at zero matric suction, and α, m and n are fitting parameters that are related to the pore size and pore size distribution of the soil.

Figure 3 plots the variations of the net horizontal stress, σ_{h}, versus the net vertical stress, σ_{v}, for different soil specimens. In addition, the variations of the void ratio of the soil, e, versus net vertical stress, σ_{v}, are shown in Fig. 4. In this research, a series of complementary tests were performed for all specimen groups under zero matric suction to develop the proposed DSC model under fully saturated conditions. Results from the complementary tests under zero matric suction conditions are also plotted in Figs. 2 and 3.

4 Calculation of model parameters

Based on the constitutive relationships mentioned in previous sections and the use of experimental data reported by Pirjalili et al. [41], the following steps were followed calculate the variations of the unsaturated coefficient of the

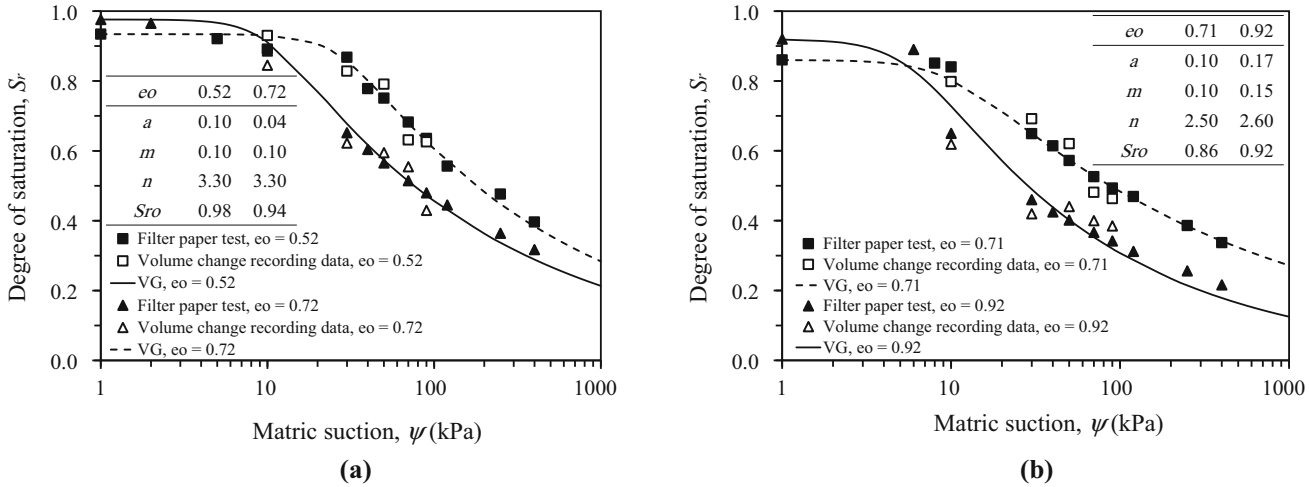

Fig. 2 SWRC of the examined soils: **a** Sand–Kaolin mixture and, **b** Firouzkouh Clay [41]

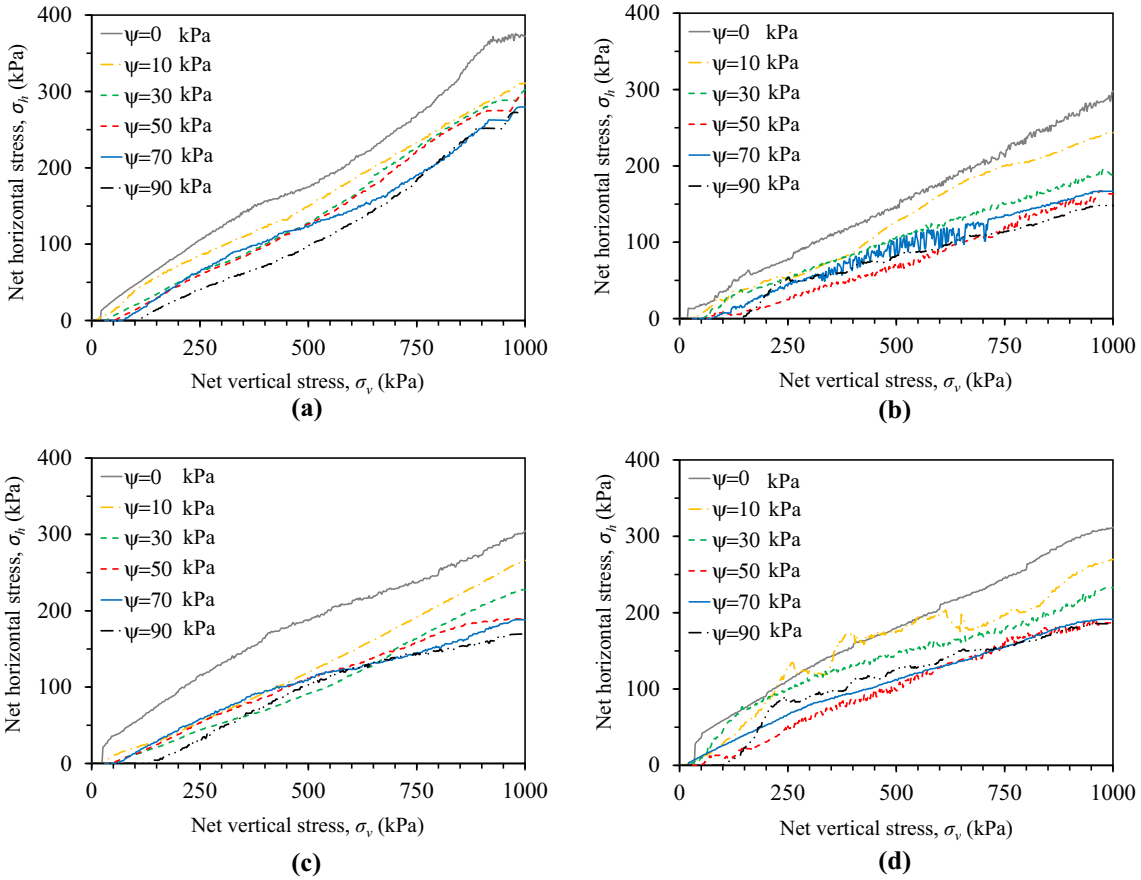

Fig. 3 Variations of the net horizontal stress, σ_h, versus the net vertical stresses, σ_v, for: **a** Sand–Kaolin mixture with e_o = 0.52, **b** Sand–Kaolin mixture, e_o = 0.72, **c** Firouzkouh Clay, e_o = 0.71 and **d** Firouzkouh Clay, e_o = 0.92 [41]

lateral soil pressure, k, against the effective vertical stress, σ_v':

4.1 Step 1: Considering input data

The input data sets that were considered to determine the parameters of the proposed DSC model are the SWRC of the proposed unsaturated soil under the wetting path

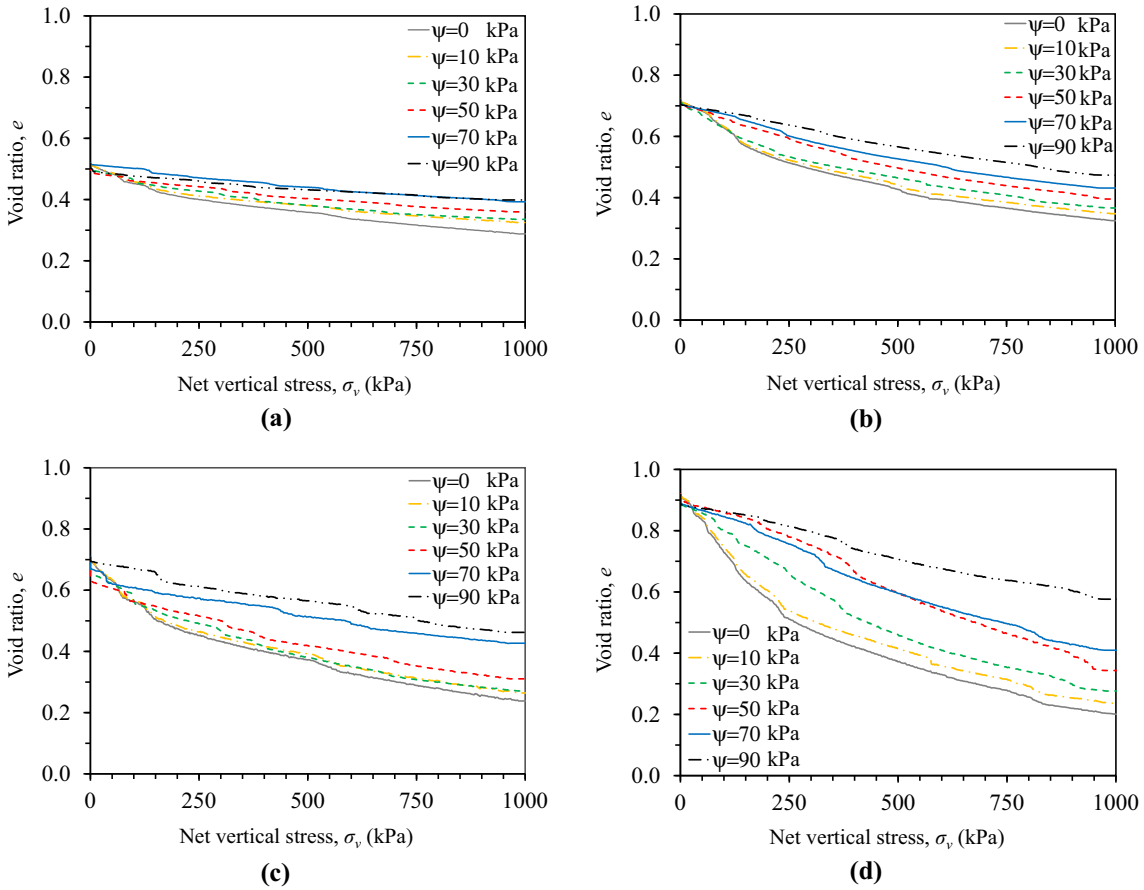

Fig. 4 Variation of the void ratio, e, versus net vertical stress, σ_v, for: **a** Sand–Kaolin mixture, e_o = 0.52, **b** Sand–Kaolin mixture, e_o = 0.72, **c** Firouzkouh Clay, e_o = 0.71 and **d** Firouzkouh Clay, e_o = 0.92 [41]

(Fig. 2), variation of σ_h versus σ_v (Fig. 3), and variations of e versus σ_v (Fig. 4).

4.2 *Step 2: Calculation of effective vertical and horizontal stresses (σ'_v and σ'_h)*

Since the coefficient of the lateral soil pressure is generally defined as the ratio of the effective horizontal stress to the effective vertical stress (as previously shown by Eq. 1), the variations of σ'_h versus σ'_v were calculated using Eqs. (2) and (3) and considering net horizontal and vertical stress data, as plotted in Figs. 2 and 3. In addition, the effective stress parameter, χ, was considered equal to the degree of saturation of the soil, S_r, as suggested by Wheeler et al. [4, 43, 48].

4.3 *Step 3: Calculation of the coefficients of lateral soil pressure at FA and RI states (k_{FA} and k_{RI})*

As previously mentioned, the two upper and lower structural disturbance states of unsaturated soils, *FA* and *RI* states, can be taken as the soils states at the minimum and the maximum applied matric suction conditions, respectively. Accordingly, in this research, data presented for ψ = 0 kPa and ψ = 90 kPa were considered as *FA* and *RI* data sets, respectively. Variations of σ'_h versus σ'_v (obtained through Step 2) are used in Eq. (1) to calculate the experimental values of k_{FA} and k_{RI}. Figure 5 illustrates variations of k_{FA}, and k_{RI} versus σ'_v for the examined soils.

4.4 Step 4: Calculation of the disturbance parameter, D

First, the four factors of ζ_v, D_u, a and z were calculated based on Eq. (5):

- *Calculation of accumulative plastic volumetric strain, ζ_v*

To calculate the accumulative plastic volumetric strain, ζ_v, the total volumetric strain, ζ_v, should be determined at each net vertical stress increment (in accordance with the data plotted in Fig. 4), and then, the share of the elastic volume strains, ζ_e, is subtracting from the total volumetric

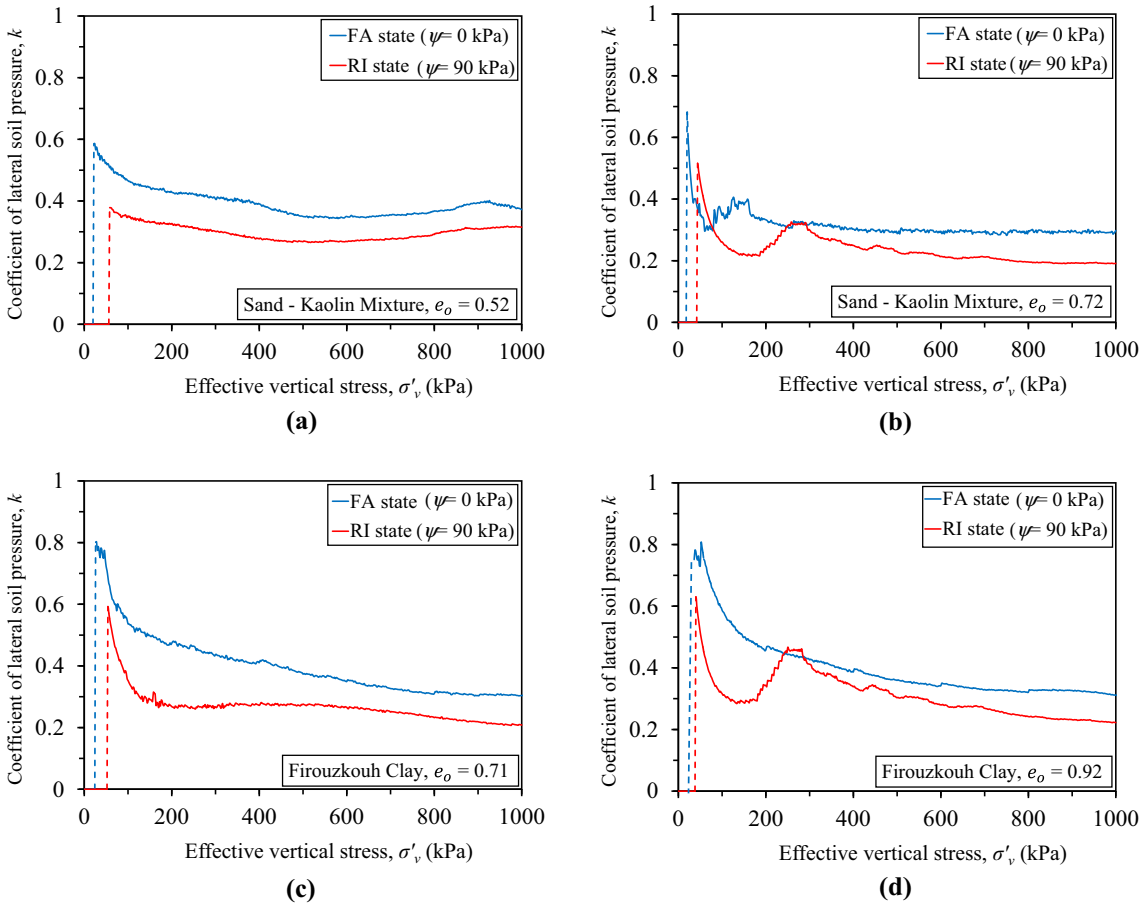

Fig. 5 Variation of k_{FA} and k_{RI} versus σ'_v for: **a** Sand–Kaolin Mixture, e_o = 0.52, **b** Sand–Kaolin Mixture, e_o = 0.72, **c** Firouzkouh Clay, e_o = 0.71 and **d** Firouzkouh Clay, e_o = 0.92 [41]

strains to obtain the plastic volumetric strain increments. Finally, ζ_v was obtained by adding the increments, $\delta\zeta_v$. The elastic volume strain is the strain that is recorded at the net vertical stress corresponding to the k_o value for each soil specimen. Using the experimental data plotted in Fig. 4, ζ_v is determined by Eq. (8):

$$\varepsilon_v = \frac{\Delta e}{1 + e_o} \tag{8}$$

In Eq. (8), Δe is the changes in void ratio, e, during each loading increment, and e_o is the initial void ratio of the examined soil specimen.

- *Calculation of D_u, a and z as suction-dependent parameters*

In this research, constitutive parameters D_u, a and z are defined in terms of soil matric suction. Actually, in unsaturated soils, these parameters are dependent on the hydromechanical responses of the soil and unsaturated state variables, such as effective stress, degree of saturation and matric suction [15]. Accordingly, Eqs. (9) to (11) are proposed in terms of the soil SWRC and decadic (*i.e.,* base 10) logarithm functions of matric suction, as:

$$D_u(\psi) = 1 - \left(\frac{S_{r(\mathrm{RI})}}{S_r(\psi)} \times \frac{\log(1+\psi)}{\log(1+\psi_{\mathrm{RI}})}\right)^{C_{\mathrm{Du}}} \tag{9}$$

$$a(\psi) = a_o \times \left(\frac{S_{r(\mathrm{RI})}}{S_r(\psi)} \times \frac{\log(1+\psi)}{\log(1+\psi_{\mathrm{RI}})}\right)^{C_a} \tag{10}$$

$$z(\psi) = z_o \times \left(\frac{S_{r(\mathrm{RI})}}{S_r(\psi)} \times \frac{\log(1+\psi)}{\log(1+\psi_{\mathrm{RI}})}\right)^{C_z} \tag{11}$$

In Eqs. (9) to (11), $S_{r(\mathrm{RI})}$ is the degree of saturation of the soil at a matric suction corresponding to *RI* condition, ψ_{RI} (ψ_{RI} = 90 kPa for the soils examined in this research) and, $S_r(\psi)$ is the degree of saturation of the soil at a given matric suction, ψ. In addition, a_o, z_o, C_{Du}, C_a and C_z are fitting parameters.

The form of the relationships presented in Eqs. (9) to (11) for calculating D_u, a and z guarantees the consistency of the stress-deformation behavior of the examined soils with the SWRC behavior of unsaturated soils and also satisfies the fundamentals of the DSC model [15]. In other

words, these equations show a continuous behavior at a matric suction range from zero to the air entry suction value of the soil (*i.e.*, fully saturated soil conditions) and also result in the maximum disturbance of the soil (with $D = 1$), which is proportional to the *FA* state of the soil. In addition, suction values higher than ψ_{RI} in Eqs. (9) to (11) result in a minimal disturbance in the soil structure and lead to $D = 0$ in a continuous manner.

4.5 Step 5: Calculation of the unsaturated coefficient of lateral soil pressure, k, in terms of effective vertical stress, σ'_v

In the final step, considering data obtained from steps 1 to 4 and implementing Eq. (6), the variation of the unsaturated coefficient of lateral soil pressure, k, at a given effective vertical stress, σ'_v, can be calculated.

Note: The DSC model proposed in this study can present the changes in the coefficient of lateral soil pressure in unsaturated soils in the form of a *continuous* mathematical function. Therefore, it provides a suitable platform for use in numerical simulations. In addition, since the model is conceptually based on changes in soil structure, it is completely consistent with what occurs in the soil under lateral loading from the at-rest to the active state. Moreover, in the proposed DSC model, the model variables are defined as a function of effective stress variables coupled with the unsaturated hydraulic parameters of the soil (*i.e.,* SWRC). Accordingly, more complicated hydromechanical stress paths can be considered to further develop the proposed model.

5 Results

Suction-dependent DSC parameters (*i.e., D_u*, *a* and *z*) were calculated for different soils by considering the constitutive relationships mentioned in the previous sections, using the experimental data reported by Pirjalili et al. [41], and following Steps 1 to 4, and the results are plotted in Fig. 6. In addition, values of parameters a_o and z_o, and variations of C_{Du}, C_a, and C_z against matric suction were calculated for different soil conditions, and the results are presented in Table 1 and Fig. 7, respectively. It should be noted that the Least Squares Method was used in this study to calculate the parameters of the DSC model to obtain the best fit between the predicted and the experimental values of the lateral pressure coefficients.

As depicted in Fig. 6, similar trends for each DSC parameter are observed against matric suction for all studied soils. Accordingly, D_u decreases as matric suction values increase so that it has a value of unity in the *FA* state (when $\psi = 0$) and then gradually decreases to zero in the *RI* state (when $\psi = 90$ kPa). Similar trends are observed for variations of a and z versus matric suction, as these parameters have zero values in the *FA* state and then gradually reached their maximum values (a_o and z_o, respectively) in the *RI* state. Figure 6 also shows that for a given soil type, larger a and z parameters are obtained for specimens with the lower initial void ratios in comparison with looser samples. In contrast, larger D_u values were obtained for specific soil type specimens with higher initial void ratios than dense specimens, which implies a higher structural disturbance potential in looser soil specimens. Moreover, Table 1 suggests that the values of a_o and z_o depend on the soil type and the initial void ratio of the soil. Therefore, we deduce that for each type of soil, a_o and z_o have greater values at lower initial void ratios in comparison with the loose samples.

Data presented in Fig. 7 show that parameters C_{Du}, C_a and C_z decrease as the matric suction increases. In C_a and C_z, this reduction continues until their values reach zero at high matric suctions. In addition, it is observed that C_{Du}, C_a and C_z have greater values for the specimens with higher initial void ratios in comparison with dense soil specimens.

The variation of the unsaturated coefficient of lateral soil pressure, k, is calculated by considering experimental data reported by Pirjalili et al. [41], implementing the calculated values of k_{FA} and k_{RI} as shown in Fig. 5, considering values of C_{Du}, C_a, C_z and D_u, z, a, as presented by Figs. 6 and 7, and following Step 5; it is illustrated in terms of the effective vertical stress, σ'_v, in Figs. 8 and 9 for Sand–Kaolin Mixture and Firouzkouh Clay specimens, respectively. Corresponding experimental values of k against σ'_v are also plotted for comparison in Figs. 8 and 9. Accordingly, very good agreement is observed between the model predictions and the experimental data.

Note: Effective stress values recorded by implemented sensors have shown irregular fluctuations and jumps during the experimental work and at the beginning of the loading stages, and this might be due to instrument errors at very low stress values, inter-particle rearrangement within the soil texture, and initiation of stress–strain mobilization. These fluctuations were also observed in variations of the lateral soil pressure versus effective vertical stress before the soil reached its maximum lateral soil pressure (*i.e.,* its at-rest state). Since the mathematical description and conceptual interpretation of these irregularities were not possible using the proposed DSC framework, the mentioned jumps and fluctuations are replaced with vertical dashed-lines according to their general trends in Figs. 8 and 9.

Data illustrated in Figs. 8 and 9 indicate that k grows rapidly after increasing the effective vertical stress up to a maximum in the early stages of loading and then decreases to an asymptotic value. In Figs. 8 and 9, the maximum value of k represents the unsaturated at-rest coefficient of

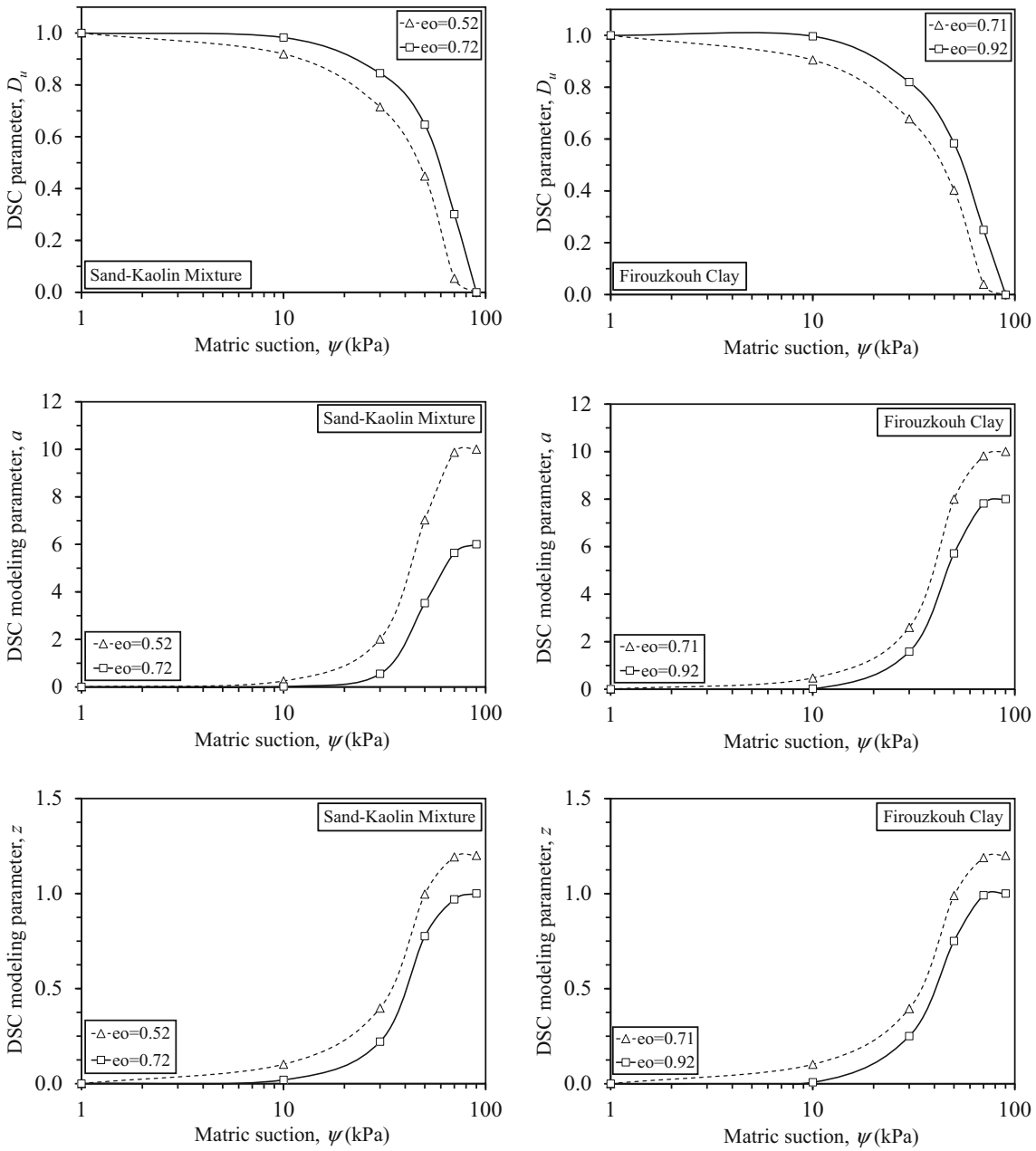

Fig. 6 Variations of D_u, a and z versus matric suction, ψ, for the examined soils

Table 1 Suggested values for a_o and z_o for the examined soils

Parameter	Sand–Kaolin mixture		Firouzkouh Clay	
	e_o = 0.52	e_o = 0.72	e_o = 0.71	e_o = 0.92
a_o	10	6	10	8
z_o	1.2	1	1.2	1

the lateral soil pressure, k_o. By further increasing the effective vertical stress and surpassing the at-rest condition, the lateral deformations within the soil mass increase, and k continually decreases until the soil reaches its active limit state of failure and k asymptotically approaches its corresponding active value, k_a.

6 Analysis and discussion

In this section, the validity of the proposed DSC model is assessed by making a quantitative comparison between the experimental and model-predicted k values. To this end, the Root Mean Square Error (*RMSE*) and the Normalized Root Mean Square Error (*NRMSE*) parameters are

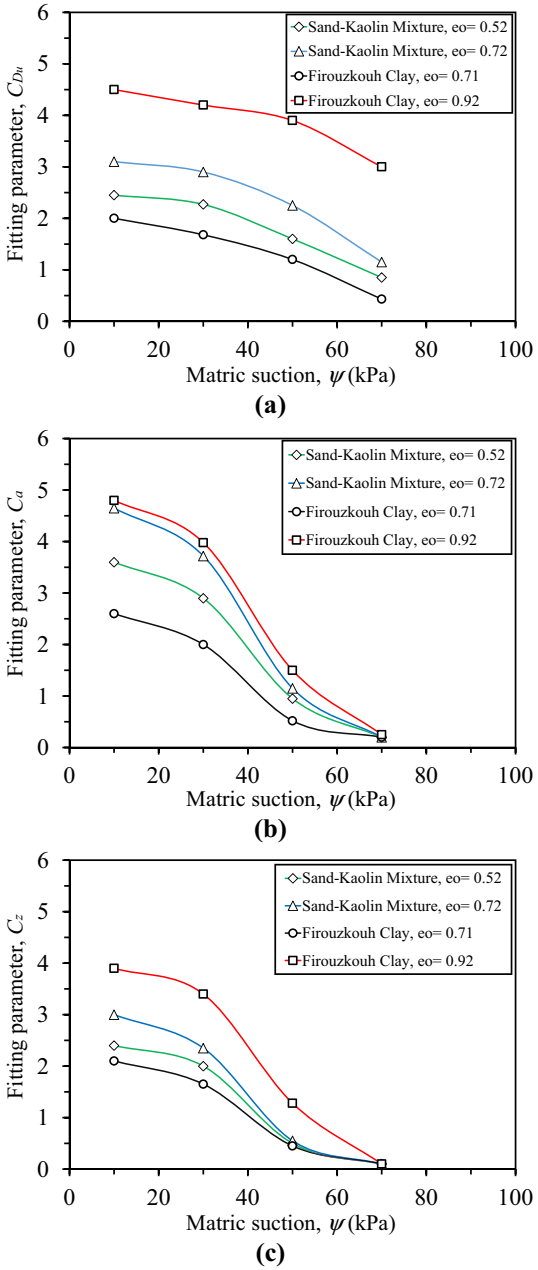

Fig. 7 Variations of: **a** C_{Du}, **b** C_a and **c** C_z versus matric suction, ψ, for the examined soils

calculated for comparative data sets by implementing Eqs. (12) and (13):

$$\mathrm{RMSE} = \sqrt{\frac{\sum_{i=1}^{N}\left(k_{\mathrm{experimental}} - k_{\mathrm{predicted}}\right)^2}{N}} \tag{12}$$

$$\mathrm{NRMSE} = \frac{\mathrm{RMSE}}{\mathrm{Max}\left(k_{\mathrm{experimental}}\right) - \mathrm{Min}\left(k_{\mathrm{experimental}}\right)} \tag{13}$$

In Eq. (12), $k_{\mathrm{experimental}}$ and $k_{\mathrm{predicted}}$ are the experimental and model-predicted values of k, respectively, N is number of data in each data set and i is the numeral. In addition, in Eq. (13), Max($k_{\mathrm{experimental}}$) and Min($k_{\mathrm{experimental}}$) are the maximum and minimum values of the experimental values of k, respectively. Calculated values of RMSE and NRMSE parameters are shown in Table 2 for the comparative data sets.

Data presented in Table 2 indicate that the maximum relative and normalized errors are (0.053 and 8.5%) and (0.065 and 10.2%) for the Sand–Kaolin mixture and the Firouzkouh Clay specimens, respectively.

By considering data summarized in Table 2 and taking into account Figs. 8 and 9, we see excellent conformance is obtained between the model-predictions and experimental variations of k versus effective vertical stress, σ'_{v}. In addition, the three distinct phases in variation of k versus σ'_{v}, namely the at-rest, transition and active phases, are shown to be well captured by the proposed effective stress-based DSC model.

To display the accuracy and reliability of the proposed DSC model, experimental and model-predicted values of k_o and k_a are compared in Figs. 10 and 11, respectively, along with the identity lines and corresponding R-squared values. Figures 10 and 11 clearly show that predicted and experimental data are mostly aligned with the identity lines, which implies the proposed model can predict the at-rest and active k values for the examined soils appropriately.

7 A prototype practical example

In order to demonstrate the practical functionality of the proposed DSC model, a prototype example problem of lateral soil pressure acting on a gravity retaining wall is presented under unsaturated soil conditions. In this case, soil properties were considered the same as the soil specimens in this study, with a matric suction range of zero to 90 kPa. Then, the lateral soil pressure acting on the wall in at-rest and active conditions was calculated by the proposed effective stress-based DSC model. For comparison, the corresponding values of the at-rest and active soil pressures were also calculated utilizing conventional soil mechanics concepts ignoring the unsaturated soil properties (namely *Ordinary condition*, in this section).

Note: In the prototype example problem, the exact conditions adopted in the experimental laboratory tests by Pirjalili et al. [41] have been taken into account. As in that study, the implemented ring device (in which the tested soil specimens were placed) was allowed to have lateral expansion during the tests but was fixed against rotation.

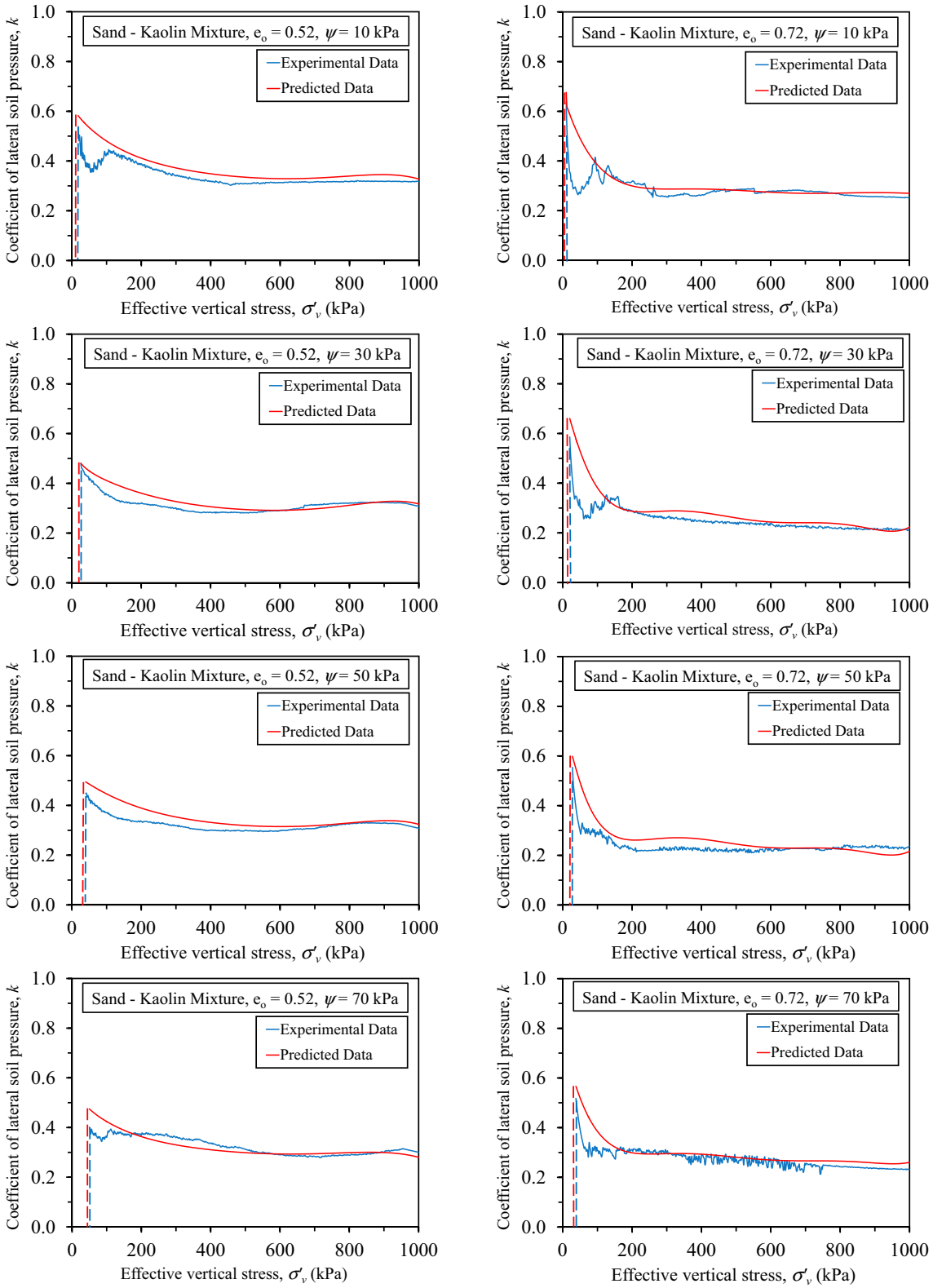

Fig. 8 Model-predictions and experimental values of k for Sand–Kaolin mixture specimens

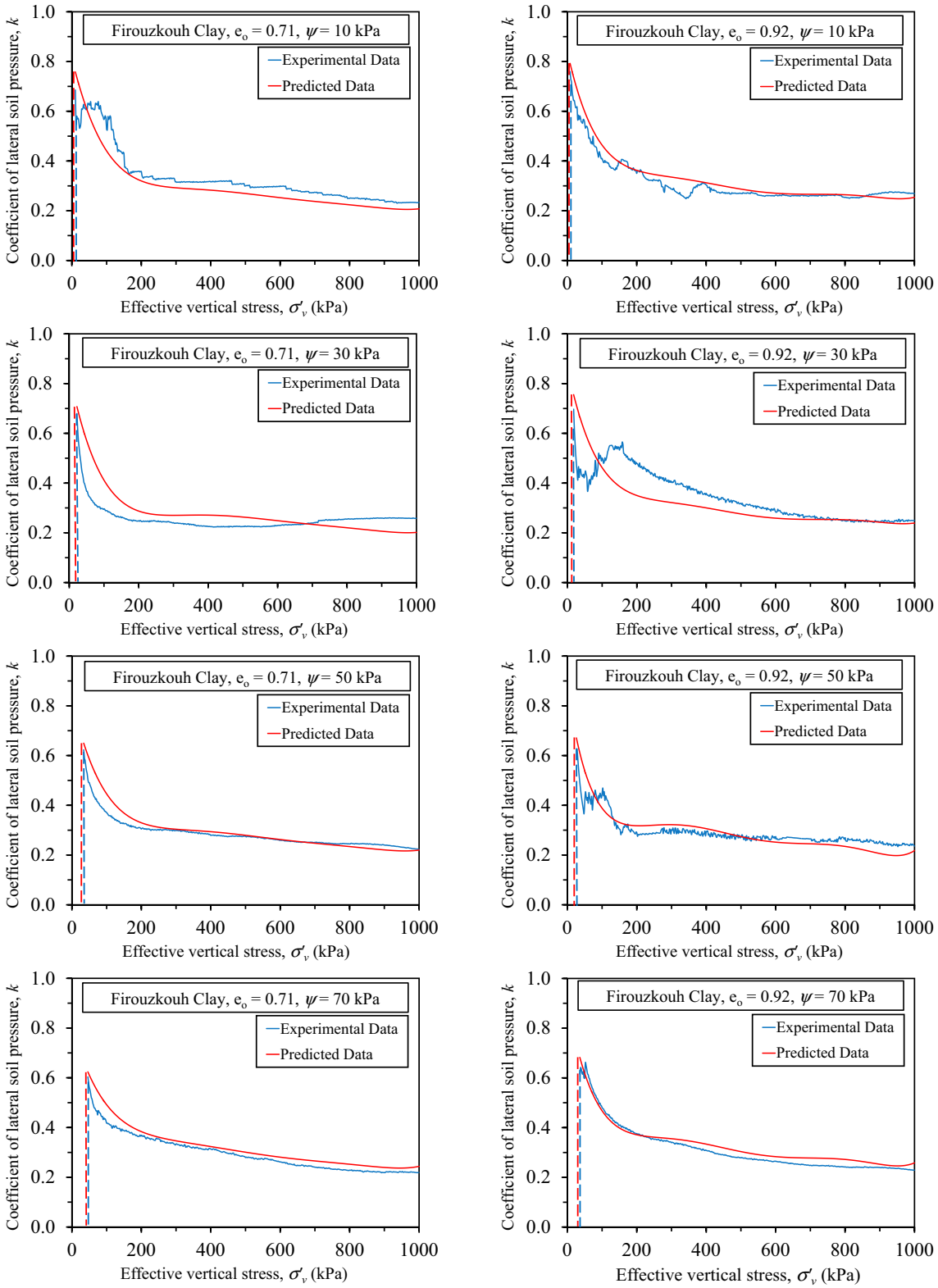

Fig. 9 Model-predictions and experimental values of k for Firouzkouh Clay specimens

Table 2 RMSE and NRMSE parameters for model-predictions and experimental k values

Soil type	Matric suction ψ (kPa)	RMSE	NRMSE (%)	RMSE	NRMSE (%)
Sand–Kaolin mixture		e_o = 0.52		e_o = 0.72	
	10	0.041	8.0	0.052	8.4
	30	0.026	5.4	0.050	8.1
	50	0.035	7.8	0.053	8.5
	70	0.038	7.9	0.049	7.9
Firouzkouh Clay		e_o = 0.71		e_o = 0.92	
	10	0.051	7.4	0.031	4.5
	30	0.06	8.2	0.065	10.2
	50	0.029	4.6	0.035	5.2
	70	0.035	5.4	0.021	3.2

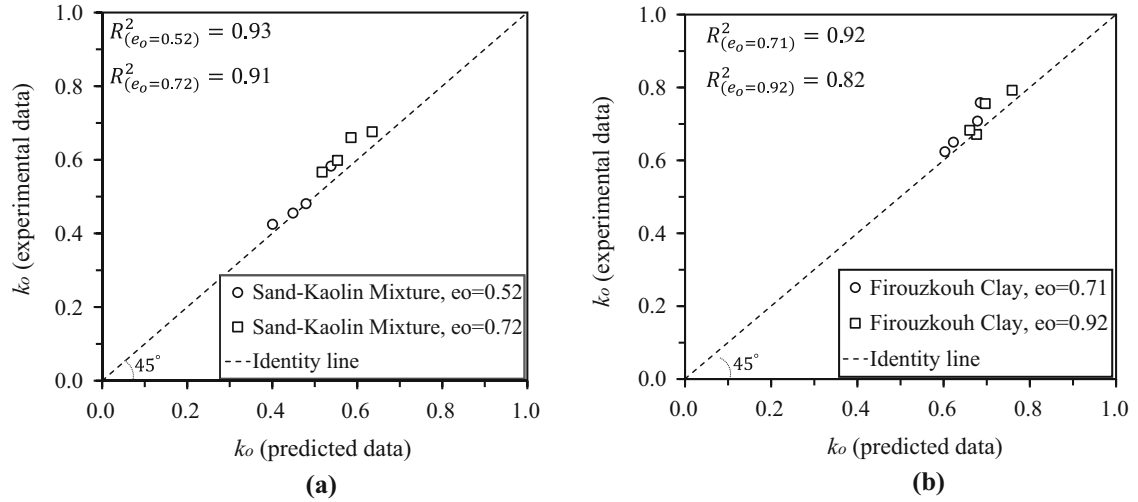

Fig. 10 Comparison between the model-predicted and experimental values of k_o for: **a** Sand–Kaolin mixture and **b** Firouzkouh Clay

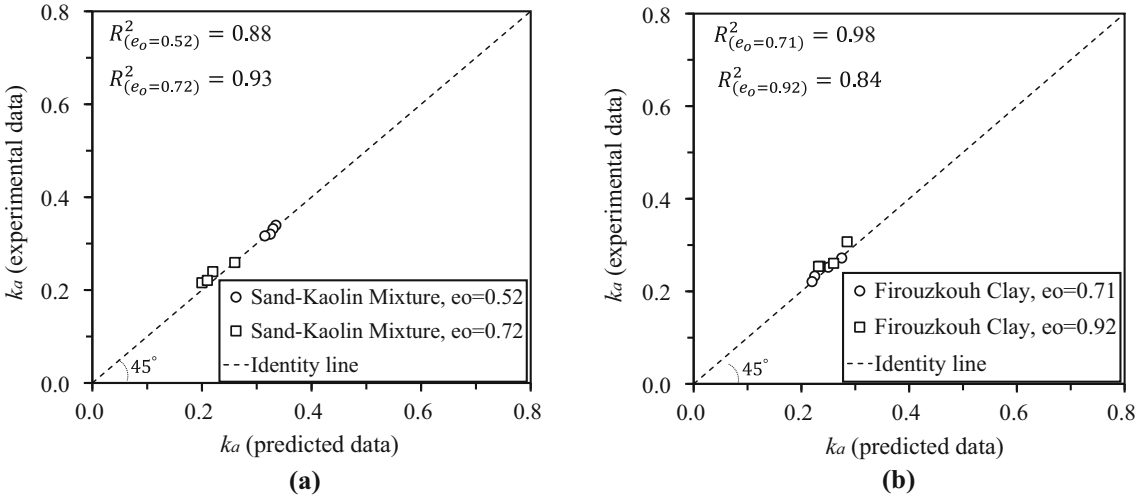

Fig. 11 Comparison between the model-predicted and experimental values of k_a for: **a** Sand–Kaolin mixture and **b** Firouzkouh Clay

Accordingly, the gravity wall in this prototype example was assumed to reach the active state by wall translation.

7.1 Example characteristics

The schematic of the proposed gravity wall is depicted in Fig. 12 with the soil condition and water level (*GWL*) location. As shown in Fig. 12, the *GWL* is located at the level of the wall foundation. It is assumed that the soil material above the ground water table is an unsaturated backfill, in which, the matric suction varies linearly from the ground water table (where $\psi = 0$) up to the ground surface, in the form of negative hydrostatic pore water pressure [32]. The wall height, h_{unst}, and the water density, γ_w, are considered 9 m and 10 kN/m^3, respectively. Accordingly, the maximum value of the matric suction within the unsaturated backfill soil is 90 kPa, which is consistent with the maximum amount of matric suction of the soils examined in this study.

7.2 Soil properties

In this example, two different conditions are considered for the backfill soil material: the *Unsaturated condition* and the *Ordinary condition*.

- *Unsaturated condition*

In the *Unsaturated condition*, the matric suction within the backfill soil is assumed to vary linearly in the form of negative hydrostatic water pressure from the *GWL* up to the ground surface. Accordingly, the degree of saturation of the soil is determined from the data provided by Fig. 2, and the soil density is calculated using conventional soil-phase relationships in a soil mechanics context. In addition, the coefficients of the lateral soil pressure in the at-rest and active states are determined from the data presented in Figs. 8 and 9, respectively.

- *Ordinary condition*

In the *Ordinary condition*, the degree of saturation and the density of the backfill materials were calculated similarly to the *Unsaturated condition*. However, in this case, the role of the matric suction on the coefficient of lateral soil pressure of the backfill materials was ignored and the coefficients of the at-rest and the active lateral soil pressures (*i.e.*, k_o and k_a, respectively) were considered for a fully saturated state of the soil, with respect to the conventional considerations in geotechnical engineering. Using the data presented in Fig. 5, values of k_o and k_a were extracted from the curves corresponds to the zero-suction condition (*i.e.,* the *FA* state of the examined soils).

Considered soil properties for the ordinary and unsaturated conditions are shown in Table 3.

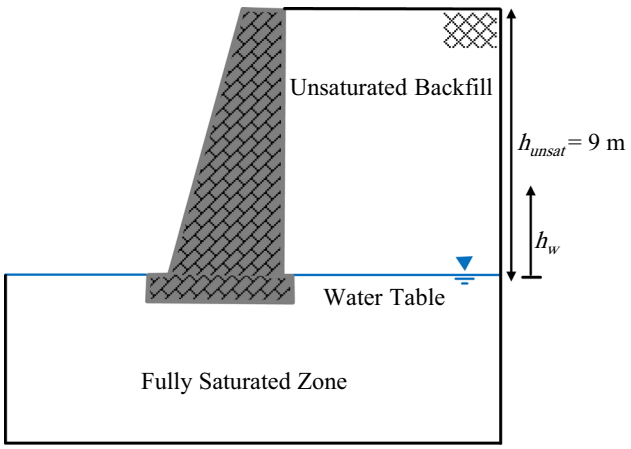

Fig. 12 Schematic of the examined gravity wall in the prototype practical example

7.3 Results

Allowing for the geometrical aspects of the studied gravity wall (as depicted in Fig. 12) and the soil properties (as given in Table 3), Eqs. (2) and (3) were used to calculate the variations of the suction-stress parameter, σ_s, net vertical stress, σ_v, and the vertical profile of the unsaturated backfill soil, the results are plotted in Fig. 13a, b, respectively. As shown in Fig. 13b, the variation of the net vertical stress of the unsaturated backfill soil versus soil height has a nonlinear form. This is due to considering the changes in matric suction of the soil versus height that has led to different degrees of saturation and bulk density in the height of the backfill soil mass.

By considering data presented in Figs. 8, 9, and 13, implementing Eq. (3a), and following the proposed DSC model, variations of the at-rest and active effective horizontal (lateral) soil pressures, σ'_h, along the unsaturated backfill soil height are calculated for the examined soils, the results are illustrated in Fig. 14. For better visual comparison, distributions of the at-rest and active effective lateral soil pressures against the backfill soil height (calculated for the ordinary state of the examined soils) are also plotted in Fig. 14. As can be seen in Fig. 14, it is evident that considering the unsaturated state for the backfill soil led to less effective lateral pressures in comparison with the corresponding ordinary cases.

From a practical point of view, the at-rest soil pressure is commonly considered in the structural design of retaining walls, while the active soil pressure is taken into account to check the wall stability versus rotation and base sliding. In this light, in the current example, the overall lateral forces, F_h, in the at-rest and active states of the backfill soil are calculated for the examined soils, and the results are

Table 3 Soil parameters in the prototype practical example

Analysis type	Soil type	e_o	G_s	ψ (kPa)	S_r	γ (kN/m^3)	k_o	k_a
Unsaturated	Sand–Kaolin mixture	0.52	2.66	Negative hydrostatic pressure	Variable (Fig. 2a)	Variable	Variable (Fig. 7)	Variable (Fig. 7)
		0.72						
	Firouzkouh Clay	0.71	2.75		Variable (Fig. 2b)		Variable (Fig. 8)	Variable (Fig. 8)
		0.92						
Ordinary	Sand–Kaolin mixture	0.52	2.66	-	Variable (Fig. 2a)	Variable	0.60	0.36
		0.72					0.70	0.36
	Firouzkouh Clay	0.71	2.75		Variable (Fig. 2b)		0.78	0.31
		0.92					0.82	0.32

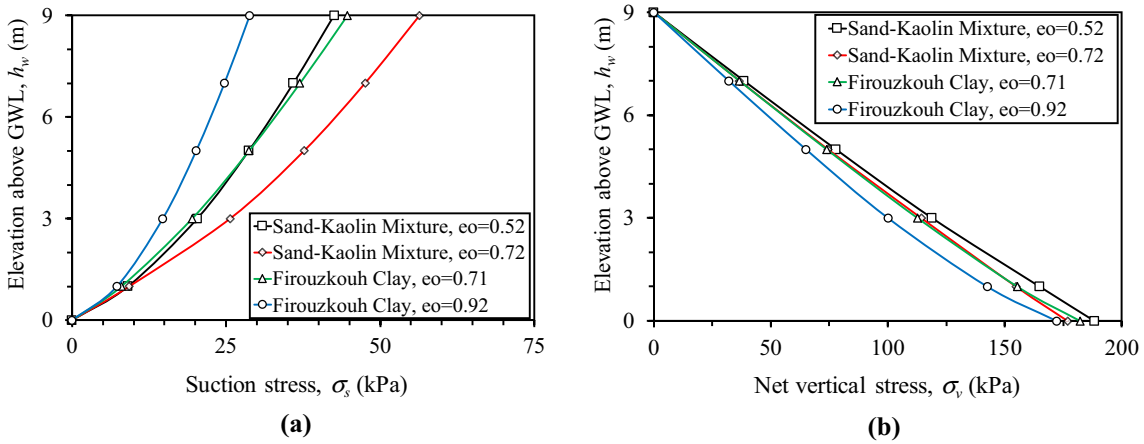

Fig. 13 The variations of the **a** suction stress, σ_s, and **b** net vertical stress, σ_v, versus soil elevation above GWL, h_w

plotted in Fig. 15 for both cases of unsaturated and ordinary states.

With respect to the data plotted in Fig. 15, it is observed that considering the unsaturated state for the backfill soil resulted in an average reduction of 10.1% and 10.4% in total lateral forces acting on the wall in the at-rest and active states, respectively. This means that considering unsaturated parameters for backfill soil results in more economical and precise design procedures for retaining walls.

8 Conclusion

In this paper, an analytical approach has been introduced for calculating the unsaturated coefficient of lateral soil pressure, k, based on the disturbed state concept (DSC) in conjunction with an effective stress approach for unsaturated soils. In terms of the soil matric suction, the parameters of the proposed model have been defined as SWRC-compatible functions. Experimental data reported in [41] for two different soil types, a Sand–Kaolin Mixture and Firouzkouh Clay (each had two different initial void ratios and were tested under five applied matric suctions), have been used along with four complimentary fully saturated tests to calculate the parameters of the proposed model.

The lower and upper boundaries for the structural disturbance characteristics of the examined soils (*i.e.*, fully adjusted and relative intact conditions, respectively) have been defined to calculate the disturbance parameter, D. The proposed model was shown to be capable of properly predicting the unsaturated coefficient of lateral soil pressure values, k, under increasing effective vertical stress and for different state variables and soil parameters (*i.e.,* the matric suction and initial void ratio). k values measured under the minimum and maximum applied matric suction (*i.e.*, ψ = zero and ψ = 90 kPa) were used to calculate the unsaturated coefficient of the lateral soil pressures at the lower and upper structural disturbance boundaries. In addition, the vertical and horizontal stress state parameters have been defined in accordance with the single-phase Bishop's effective stress approach for unsaturated soils.

Quantitative comparisons made between the model predictions and experimental values of k revealed the

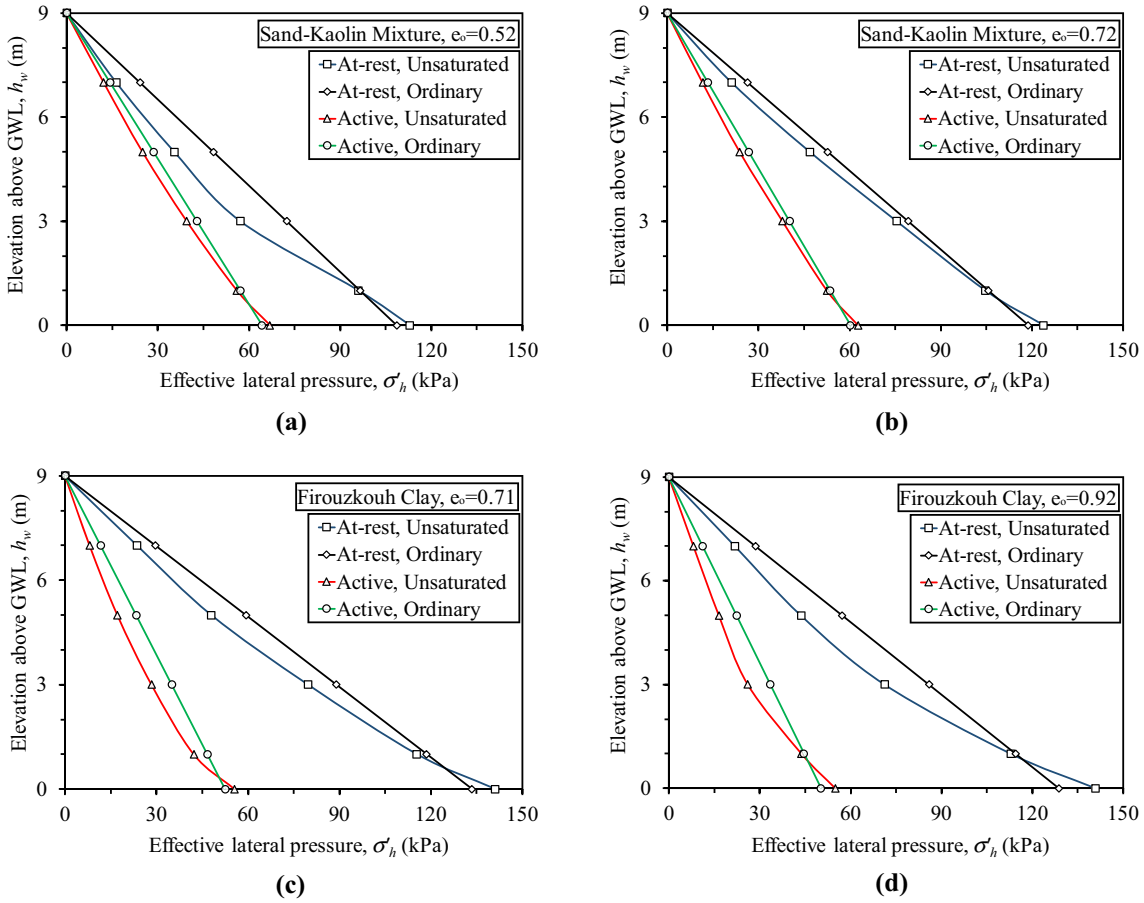

Fig. 14 Distribution of the at-rest and active lateral soil pressure in unsaturated and ordinary states for: **a** Sand–Kaolin mixture, e_o = 0.52, **b** Sand–Kaolin mixture, e_o = 0.72, **c** Firouzkouh clay, e_o = 0.71 and **d** Firouzkouh Clay, e_o = 0.92

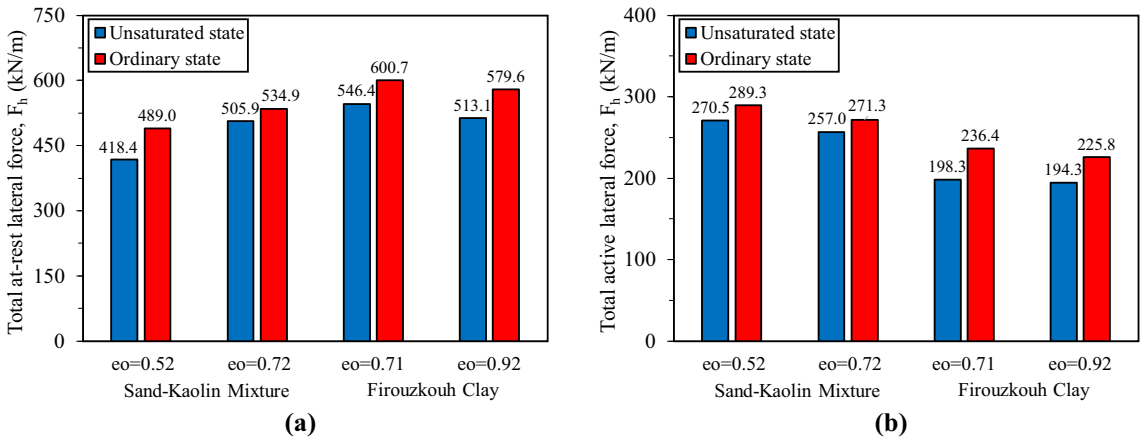

Fig. 15 Total lateral forces act on the wall in unsaturated and ordinary conditions of the examined soils for: **a** at-rest state and **b** active state

excellent validity of the proposed effective stress-based DSC model for predicting the continuous variations of the unsaturated coefficient of lateral soil pressure against increasing effective vertical stress, from the at-rest to the active state of the examined soils. Accordingly, *NRMSE* values ranging from 3.2% to 10.2% have been obtained for the model-predicted and experimental data sets. Moreover, it has been found that the disturbance parameter, *D*, of the examined unsaturated soils is considerably affected by the soil matric suction and initial void ratio.

Finally, in order to evaluate the performance of the proposed model for engineering problems, a practical

example of calculation of lateral soil pressures act on a gravity wall (under conditions and specifications corresponding to the properties of the soils studied in this research) has been solved, and the values of the lateral forces acting on the wall in the at-rest and active states of the backfill soil have been calculated. Accordingly, two different conditions, namely, unsaturated (for the proposed model) and ordinary conditions (for conventional geotechnical engineering), were considered for the backfill soil materials. Quantitative comparisons between the obtained results indicate that the proposed DSC model not only led to more precise values of the lateral forces acting on the retaining walls (due to the use of more realistic soil conditions) but also reduced the project costs since it has resulted in lower values for design loads.

Acknowledgements The experimental work that is referred in this research was performed at Tarbiat Modares University, as a part of the MSc thesis of the second author. The authors of this paper deeply acknowledge the supports of Tarbiat Modares University. In addition, the first author would like to appreciate the Niroo Research Institute for providing him with the opportunity to contribute in this research. Also, the authors would like to thank Mrs. Shari Holderread for her diligence proofreading of this paper.

Funding This research received no specific grant from any funding agency in the public, commercial, or not-for-profit sectors.

Data availability The datasets generated or analyzed during the current study are available from the corresponding author upon reasonable request.

Code availability Not applicable.

Declarations

Conflict of interest The authors declare that they have no known competing financial interests or personal relationships that could have appeared to influence the work reported in this paper.

References

1. Abrantes LG, Pereira de Campos TM (2019) Evaluation of the coefficient of earth pressure at rest (K0) of a saturated-unsaturated colluvium soil A. In: Tarantino, Ibraim E (eds) E3S web of conferences, vol 92, p 07006. https://doi.org/10.1051/e3sconf/20199207006
2. Bishop AW (1959) The principle of effective stress. Teknisk ukeblad 39:859–863
3. Bishop AW, Henkel D (1957) The measurement of soil properties in the triaxial test. E. Arnold, London
4. Borja RI (2004) Cam-clay plasticity. Part V: a mathematical framework for three-phase deformation and strain localization analyses of partially saturated porous media. Comp Met Appl Mech Eng 193(48–51):5301–5338. https://doi.org/10.1016/j.cma.2003.12.067
5. Chu J, Gan C (2004) Effect of void ratio on ko of loose sand. Géotechnique 54(4):285–288. https://doi.org/10.1680/geot.2004.54.4.285
6. Desai CS (1974) A consistent finite element technique for work-softening behavior. In: Oden JT (ed) Proceedings of the international conference on computational methods in nonlinear mechanics. Univ. of Texas, Austin
7. Desai CS (1994) Hierarchical single surface and the disturbed state constitutive models with emphasis on geotechnical application. In: Saxeng KR (ed) Geotechnical engineering: emerging trend in design and practice, vol 32(3). Oxford IBH Publishing Company, New Delhi, pp 115–154. https://doi.org/10.1016/0148-9062(95)90125-o
8. Desai CS (1995) Constitutive modeling using the disturbed state as a microstructure self-adjustment concept. In: Mühlhaus HB (ed) Continuum models for material with microstructure, vol 8. Wiley, London
9. Desai CS (2001) Mechanics of materials and interfaces: the disturbed state concept. CRC Press, Boca Raton. https://doi.org/10.1201/9781420041910.ch2
10. Desai CS (2015) Constitutive modeling of materials and contacts using the disturbed state concept. Part 1: background and analysis. J Comput Struct 146:214–233. https://doi.org/10.1016/j.jrmge.2016.01.003
11. Desai CS (2015) Constitutive modeling of materials and contacts using the disturbed state concept. Part 2: validations at specimen and boundary value problem levels. J Comput Struct 146:234–251. https://doi.org/10.1016/j.jrmge.2016.01.003
12. Desai CS (2016) Disturbed state concept as unified constitutive modeling approach. J Rock Mech Geotech Eng 8(3):277–293. https://doi.org/10.1016/j.jrmge.2016.01.003
13. Fathipour H, Siahmazgi AS, Payan M, Chenari RJ (2020) Evaluation of the lateral earth pressure in unsaturated soils with finite element limit analysis using second-order cone programming. Comput Geotech 125:103587. https://doi.org/10.1016/j.compgeo.2020.103587
14. Garakani AA (2013) Laboratory assessment of the hydro-mechanical behavior of unsaturated undisturbed collapsible soils—case study: Gorgan loess. Dissertation for Doctoral Degree, Sharif University of Technology, Tehran, Iran
15. Garakani AA, Haeri SM, Desai CS, Seyed Ghafouri SMH, Sadollahzadeh B, Hashemi Senejani H (2019) Testing and constitutive modeling of lime-stabilized collapsible loess. II: Modeling and validations. ASCE Int J Geomech 19(4):04019007. https://doi.org/10.1061/(ASCE)GM.1943-5622.0001386
16. Garakani AA, Haeri SM, Khosravi A, Habibagahi G (2015) Hydro-mechanical behavior of undisturbed collapsible loessial soils under different stress state conditions. Eng Geol 195:28–41. https://doi.org/10.1016/j.enggeo.2015.05.026
17. Geiser F, Laloui L, Vulliet L, Desai CS (1997) Disturbed state concept for constitutive modeling of partially saturated porous materials. In: Proceedings of the 6th international symposium on numerical models in geomechanics, Balkema, Rotterdam, Netherlands, pp 129–134
18. van Genuchten MT (1980) A closed-form equation for predicting the hydraulic conductivity of unsaturated soils. Soil Sci Soc Am J 44(5):892–898. https://doi.org/10.2136/sssaj1980.03615995004400050002x
19. Haeri SM, Garakani AA, Khosravi A, Meehan CL (2014) Assessing the hydro-mechanical behavior of collapsible soils using a modified triaxial test device. ASTM Geotech Test J 37(2):190–204. https://doi.org/10.1520/GTJ20130034
20. Haeri SM, Garakani AA, Roohparvar HR, Desai CS, Seyed Ghafouri SMH, Kouchesfahani KS (2019) Testing and constitutive modeling of lime-stabilized collapsible loess. I: Experimental investigations. ASCE Int J Geomech 19(4):4019006. https://doi.org/10.1061/(ASCE)GM.1943-5622.0001364
21. Haeri SM, Khosravi A, Garakani AA, Ghazizadeh S (2017) Effect of soil structure and disturbance on hydromechanical

behavior of collapsible loessial soils. ASCE Int J Geomech 17(1):04016021. https://doi.org/10.1061/(ASCE)GM.1943-5622.0000656
22. Jacky J (1944) The coefficient of earth pressure at rest. In: Hungarian (A nyugalmi nyomas tenyezoje), J Soc Hung Eng Arch (Magyar Mernok es Epitesz-Egylet Konzlonye), pp 355–358
23. Jacky J (1948) Pressure in Soils. Proceeding of the 2nd International Conference on Soil Mechanic and Foundation Engineering. Rotterdam, Netherlands, pp 107–130
24. Khalili N, Khabbaz MH (1998) A unique relationship for χ for the determination of the shear strength of unsaturated soils. Géotechnique 48(5):681–687. https://doi.org/10.1680/geot.1998.48.5.681
25. Khalili N, Zargarbashi S (2010) Influence of hydraulic hysteresis on effective stress in unsaturated soils. Géotechnique 60(9):729–734. https://doi.org/10.1680/geot.09.T.009
26. Kumar Thota S, Duc Cao T, Vahedifard F (2021) Poisson's ratio characteristic curve of unsaturated soils. J Geotech Geoenviron 147(1):04020149. https://doi.org/10.1061/(ASCE)GT.1943-5606.0002424
27. Li J, Xingand T, Hou Y (2014) Centrifugal model test on the at-rest coefficient of lateral soil pressure in unsaturated soils. CRC Press, Perth, pp 931–936
28. Li ZW, Yang XL (2018) Active earth pressure for soils with tension cracks under steady unsaturated flow conditions. Can Geotech J 55(12):1850–1859. https://doi.org/10.1139/cgj-2017-0713
29. Li Z, Yang X (2019) Three-dimensional active earth pressure for retaining structures in soils subjected to steady unsaturated seepage effects. Acta Geotech. https://doi.org/10.1007/s11440-019-00870-2
30. Liang WB, Zhao JH, Li Y, Zhang CG, Wang S (2012) Unified solution of Coulomb's active earth pressure for unsaturated soils without crack. Appl Mech Mater 170:755–761
31. Lu N, Godt J, Wu D (2010) A closed-form equation for effective stress in unsaturated soil. Water Resour 46:W05515. https://doi.org/10.1029/2009WR008646
32. Lu N, Likos WJ (2004) Unsaturated soil mechanics. Wiley, New York
33. Lu N, Likos WJ (2006) Suction stress characteristic curve for unsaturated soil. ASCE J Geotech Geoenviron 132(2):131–142. https://doi.org/10.1061/(ASCE)1090-0241(2006)132:2(131)
34. Mayne PW, Kulhawy FH (1982) Ko-OCR relationships in soil. J Geotech Eng Div 108(6):851–872. https://doi.org/10.1061/ajgeb6.0001306
35. Mesri G, Hayat T (1993) The coefficient of earth pressure at rest. Can Geotech J 30(4):647–666. https://doi.org/10.1139/t93-056
36. Monroy R, Zdravkovic L, Ridley A (2014) Evaluation of an active system to measure lateral stresses in unsaturated soils. ASTM Geotech Test J 37(1):1–14. https://doi.org/10.1520/GTJ20130062
37. Northcutt S, Wijewickreme D (2013) Effect of particle fabric on the coefficient of lateral soil pressure observed during one-dimensional compression of sand. Can Geotech J 50(5):457–466. https://doi.org/10.1139/cgj-2012-0162
38. Nuth M, Laloui L (2008) Effective stress concept in unsaturated soils: clarification and validation of a unified framework. Int J Numer Anal Met 32(7):771–801. https://doi.org/10.1002/nag.645
39. Oh S, Lu N, Kim T, Lee Y (2013) Experimental validation of suction stress characteristic curve from nonfailure triaxial k_o consolidation tests. ASCE J Geotech Geoenviron 139(9):1490–1503. https://doi.org/10.1061/(ASCE)GT.1943-5606.0000880
40. Okochi Y, Tatsuoka F (1984) Some factors affecting k_o values of sand measured in triaxial cell. Soils Found 24(3):52–68. https://doi.org/10.3208/sandf1972.24.3_52
41. Pirjalili A, Garakani AA, Golshani A, Mirzaii A (2020) A suction-controlled ring device to measure the coefficient of lateral soil pressure in unsaturated soils. Geotech Test J 43(6):1379–1396. https://doi.org/10.1520/GTJ20190099
42. Pirjalili A, Golshani A, Mirzaii A (2016) Experimental study on the coefficient of lateral soil pressure in unsaturated soils. In: E3S web of conferences, EDP sciences, vol 9, p 05003. https://doi.org/10.1051/e3sconf/20160905003
43. Schrefler BA (1984) The finite element method in soil consolidation. Doctoral dissertation, University College of Swansea, UK
44. Shahrokhabadi S, Vahedifard F, Ghazanfari E, Foroutan M (2019) Earth pressure profiles in unsaturated soils under transient flow. Eng Geol 260:105218. https://doi.org/10.1016/j.enggeo.2019.105218
45. Silva TA, Delcourt RT, de Campos TM (2017) Study of the coefficient of at-rest earth pressure for unsaturated residual soils with different weathering degrees. PanAm Unsaturated Soils. https://doi.org/10.1061/9780784481707.045
46. Terzaghi K (1920) Old earth-pressure theories and new test results. Eng News Rec 85(14):632–637
47. Vahedifard F, Leshchinsky BA, Mortezaei K, Lu N (2015) Active earth pressures for unsaturated retaining structures. ASCE J Geotech Geoenviron 141(11):04015048. https://doi.org/10.1061/(ASCE)GT.1943-5606.0001356
48. Wheeler SJ, Sharma RS, Buisson MSR (2003) Coupling of hydraulic hysteresis and stress–strain behaviour in unsaturated soils. Géotechnique 53(1):41–54. https://doi.org/10.1680/geot.2003.53.1.41
49. Yang HP, Xiao J, Zhang GF, Zhang R (2011) Experimental study on ko coefficient of Ningming unsaturated expansive soil. In Proceedings of the 5th international conferene on unsaturated soils, vol 1, pp 397–401
50. Zhang X, Alonso EE, Casini F (2016) Explicit formulation of at-rest coefficient and its role in calibrating elasto-plastic models for unsaturated soils. Compu Geotech 71:56–68. https://doi.org/10.1016/j.compgeo.2015.08.012
51. Zhang R, Zheng JL, Yang HP (2009) Experimental study on K0 consolidation behavior of recompacted unsaturated expansive soil. In: Recent advancement in soil behavior, in situ test methods, pile foundations, and tunneling: selected papers, from the 2009 GeoHunan international conference, pp 27–32. https://doi.org/10.1061/41044(351)5